Reflow of supported sub-100 nm polymer films as a characterization process for Nano Imprint lithography

Tanguy Lévéder, Etienne Rognin, Stéfan Landis, Laurent Davoust

Reflow of supported sub-100 nm polymer films as a characterization process for NanoImprint lithography

T. Leveder [a], E. Rognin [a,*], S. Landis [a], L. Davoust [b]

[a] CEA-LETI-Minatec, 17 rue des martyrs, 38054 Grenoble Cedex 9, France
[b] CNRS-LEGI, 17 rue des martyrs, 38054 Grenoble Cedex 9, France

In this paper, we address the reflow behavior of polymer thin films, focusing our effort on the accuracy of surface shape recognition. Although much work was already performed to control resist reflow during lens manufacturing for instance, our approach is significantly different since no contact line (substrate/polymer/atmosphere) needs to be considered. Here, a linear stability approach is successfully developed to describe the thin film evolution which is also compared with experiments. Polystyrene films, with thickness ranging from few tens of nanometers up to several hundred of nanometers were patterned with NanoImprint lithography technique. Atomic force microscopy measurements were used to characterize smooth or steep shapes, respectively. Mechanical measurements of earlier stages of pattern reflow were directly accessible without any assumption, contrary to the diffraction method usually employed. We show that by controlling the reflow process of any complex surface shape during the course of time, measurements of material parameters such as thin film viscosity, surface tension, or even Hamaker constant can be made possible.

1. Introduction

Surface dynamics of viscous polymer films have been widely studied for fundamental purposes [1] and microelectronics applications as well [2,3]. Ultra-thin film manufacturing appears to be a key point of nanotechnology engineering and numerous studies have been recently led in order to exhibit driving parameters of viscous smoothing dynamics of a nanopatterned thin film. Characterization of flow properties of polymer melts at macroscopic scale is easily performed by classical measurement devices devoted to volume rheology. In NanoImprint Lithography (NIL) processes, resist film thickness is ranging from several tens of nanometer up to several hundred of nanometer. In such configuration, surface phenomena increasingly play a decisive role which induces significant deviation for viscous-driven flows properties. Several experimental approaches, mainly based on scattering correlation methods onto iso-dense patterns (line width = space width), have been carried out [3–6]. These techniques provide a very high time resolution, but data on shape evolution depends on ab initio geometrical models used for the diffraction analysis. To our knowledge, up to now, no study had associated detailed theoretical aspects and specific nanoscale experiments.

In this paper, we address the reflow behavior of thin polymer films, focusing our attention on the accurate detection of surface shape during the course of time. Although a large amount of work was already performed to understand and control resist reflow for lens manufacturing [7], our approach distinguishes itself from existing state of art since dynamics of the contact line (substrate/resist/atmosphere) does not need to be considered in order to model our system based on a supported thin film. An analytical solution describing the system evolution is proposed in this paper and compared with experiments. Although this work was performed on polystyrene two-dimensional patterns, our approach may be extended to any kind of viscous material and feature shapes.

2. Experiments

A low molecular weight ($M_w = 27.5\ \mathrm{kg\ mol^{-1}}$) monodisperse ($M_w/M_n < 1.06$) polystyrene (PS) solution is spin-coated onto 8 in. silicon substrates. The glass transition temperature ($T_g = 102 \pm 1\ ^\circ\mathrm{C}$) is measured by Differential Scanning Calorimetry (DSC). The thickness of coated polystyrene films ranges from $h_0 = 27$ nm up to 237 nm and is measured by ellipsometry. Polystyrene films are subsequently patterned with NIL technique [8,9] (Fig. 1). Iso-dense line gratings with a pitch ranging from 2 μm up to 8 μm are imprinted at 145 °C under a pressure of 3.18×10^5 Pa, during 300 s. The imprinted lines are 30 nm high. Contrary to standard

* Corresponding author. Tel.: +33 438780741; fax: +33 438785046.
E-mail address: etienne.rognin@cea.fr (E. Rognin).

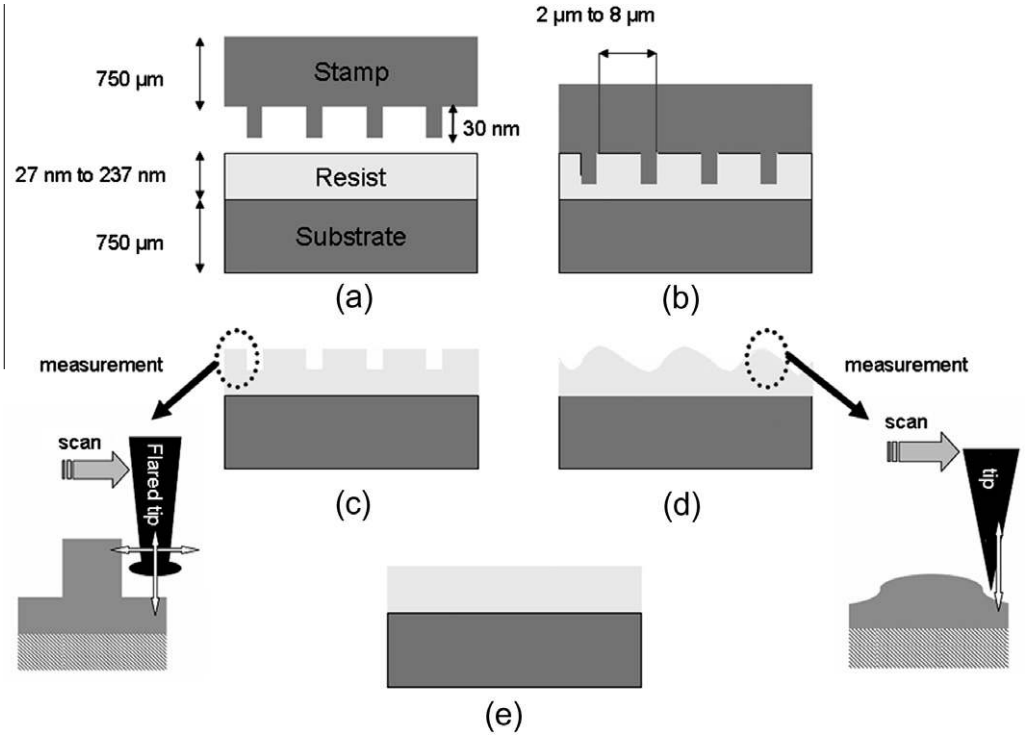

Fig. 1. NanoImprint process (a and b). Reflow experiment (c–e) and atomic force microscopy measurements with flared and conic tips.

NIL processes, the residual layer is not removed by plasma etching and resist features as-imprinted will be used in this study. Given the mold design (printed line size = spacing between two lines), the residual layer thickness is ranging from 12 nm (for $h_0 = 27$ nm) up to 222 nm (for $h_0 = 237$ nm). PS features are then annealed above T_g and cooled down to room temperature in less than one second. Patterns are further characterized by Atomic Force Microscopy (AFM) measurements performed at a spatial resolution lower than 1 nm. As previously shown [2], for the temperature range considered in this work, pattern shapes are not significantly modified by a quench. Both usual conic and flared tips [10,2] are used to characterize smooth or steep shapes, respectively (Fig. 1). Therefore, mechanical measurements of earlier stages of pattern reflow are directly made possible without any assumption, contrary to diffraction method usually employed [3].

3. Model

Pattern reflow may be seen as a process driven by a minimization of the surface free energy slowed down by the viscous shear across the polymer film [4,11]. Assuming a two dimensional pattern with a mean thickness h_0 and a surface topography characterized by the local instantaneous surface elevation $h(x,t) = h_0 + \tilde{h}(x,t)$, the reflow can be described from momentum equation completed by mass conservation equation. As shown by Oron et al. [1], due to the creeping kinetic of flow at large viscosity and the small angles thin film geometry, the momentum and mass conservation equations reduce to the Reynolds lubrication equation:

$$\partial_t h = \partial_x\left(\frac{h^3 \partial_x p}{3\eta}\right) \tag{1}$$

where $\partial_x p$ is the pressure gradient and η is the Newtonian viscosity. For nanoscopic isothermal thin films, the pressure gradient is usually created by two types of forces: the van der Waals forces (long-range molecular forces) and the surface tension [1]. It can be written as:

$$\partial_x p = \frac{A}{2\pi} \times \frac{\partial_x h}{h^4} - \gamma \times \partial_x^3 h \tag{2}$$

where A is the Hamaker constant related to the van der Waals forces in the system Si–PS–Air and γ is the surface tension. Using this expression for the pressure gradient into Eq. (1), we get:

$$\partial_t h - \frac{A}{6\pi\eta}\partial_x\left(\frac{\partial_x h}{h}\right) + \frac{\gamma}{3\eta}\partial_x\left(h^3 \partial_x^3 h\right) = 0$$

The resulting evolution equation for the thickness h is a non-linear equation which generally cannot be solved analytically. In order to obtain an analytical expression for h at any time, given any initial shape, we must linearized the evolution equation under the assumption that $\tilde{h} \ll h_0$. We get:

$$\partial_t h - \frac{A}{6\pi\eta h_0}\partial_x^2 h + \frac{\gamma h_0^3}{3\eta}\partial_x^4 h = 0 \tag{3}$$

The solving of Eq. (3) by a spectral approach is then straightforward. The thickness is expressed as a Fourier series in space whose coefficients depend on time:

$$h(x,t) = \sum_{-\infty}^{+\infty} a_n(t) \exp\left(in\frac{2\pi}{\lambda}x\right)$$

where λ is the period of the imprinted grating (or in the case of a non-periodic patterns, it is the length of the whole sample) and $a_n(t)$ is the complex amplitude of the mode n. According to Eq. (3), each Fourier mode of order n follows an exponential decay whose relaxation time τ_n is given by:

$$\frac{1}{\tau_n} = \left(n\frac{2\pi}{\lambda}\right)^2 \frac{A}{6\pi h_0 \eta} + \left(n\frac{2\pi}{\lambda}\right)^4 \frac{\gamma h_0^3}{3\eta} \tag{4}$$

Finally, the evolution of the film is described by:

$$h(x,t) = \sum_{-\infty}^{+\infty} a_n(0) \exp\left(-\frac{t}{\tau_n} + in\frac{2\pi}{\lambda}x\right) \tag{5}$$

The coefficients $a_n(0)$ are given by the Fourier transform of the initial thickness.

From Eq. (4) we can state that if the dimensionless ratio $A\lambda^2/(8\pi^3\gamma h_0^4)$ is much smaller than 1, the van der Waals forces can be clearly neglected. If we consider a typical order of magnitude for the Hamaker energy, $A = -10^{-19}$ J [12], and for the PS free surface tension $\gamma = 34$ mN m^{-1} [13], then in our experimental layout van der Waals forces have an insignificant contribution to the flow except for the largest pattern ($\lambda = 8$ μm) imprinted in the thinnest film ($h_0 = 27$ nm).

Provided that the van der Waals forces can be neglected, Eq. (4) reduces to:

$$\tau_n = \frac{3\eta}{\gamma h_0^3} \times \left(\frac{\lambda}{2\pi n}\right)^4 \tag{6}$$

Eq. (5) clearly points out the fact that the flow smoothes the high wavelengths of the film geometry.

4. Results and discussion

Fig. 2 shows AFM views of typical imprinted patterns used in this study. Fig. 3a reports the surface profile reflow at an annealing temperature of $T_g + 43$ °C of a $\lambda = 2$ μm iso-dense imprinted line array and confirms that surface effects tend to smooth the film. Iso-dense pattern is a special case where high spatial frequencies quickly disappear in favor of a monochromatic topography. It is possible to plot the decrease of the pattern height versus the annealing time (Fig. 3b). That decrease is consistent with the law of Eq. (6), and the decay time τ_1 can be extracted and the viscosity finally computed. We get $\tau_1 = 369$ s, and with $\gamma = 34$ mN m^{-1} it follows that $\eta = 3.0 \times 10^4$ Pa s.

The decay time τ_1 was easily determined from a significant height decrease of reflowed patterns. However, even for larger period and shorter corresponding annealing times, height evolution may be used to determine characteristic reflowing time more precisely. Indeed, neglecting van der Waals contribution, and using simplified Eq. (6), knowing the relaxation time τ_n, for a given profile of the initial pattern λ, it is possible to calculate the relaxation time τ_n' for any other geometry of spatial periodicity λ', because the temporal and spatial scales are directly connected. Since all arrays are iso-dense line grating, there are described by the same $a_n(t)$ coefficients. All arrays of different periods will go through the same reflowing shapes during annealing, but with different velocities. In order to compare different geometries, the time scale may be thus renormalized using the following ratio:

$$\frac{\tau(\lambda_2)}{\tau(\lambda_1)} = \left(\frac{\lambda_1}{\lambda_2}\right)^4 \tag{7}$$

We use Eq. (7) to normalize the annealing time of 4, 6 and 8 μm line gratings, respectively, to get the same time scale as the one of the 2 − μm line grating. In other words, a feature with a period $\lambda_1 = 2$ μm exhibiting a given reflow shape for an annealing time t, will present the same shape as a feature with a period λ_2 at an annealing time of t^*, provided that:

$$t^* = \left(\frac{\lambda_1}{\lambda_2}\right)^4 \times t$$

Fig. 4 represents the height evolution of patterns for normalized annealing times ranging from 0.02 s (corresponding to 50 s for

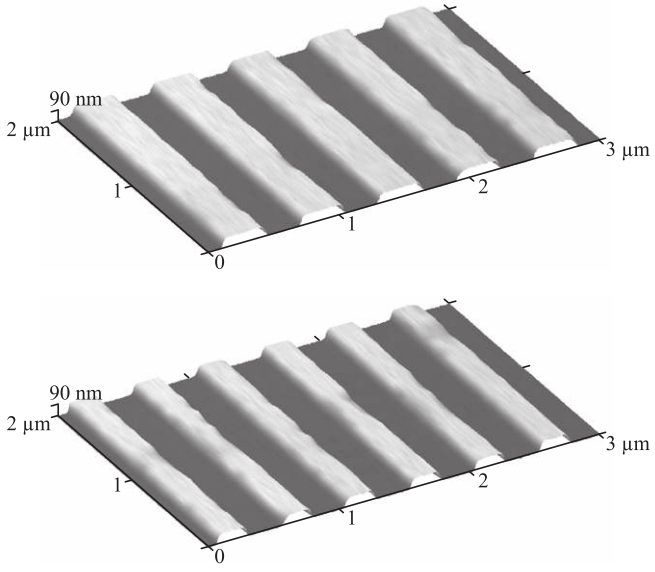

Fig. 2. AFM images of two typical imprinted patterns.

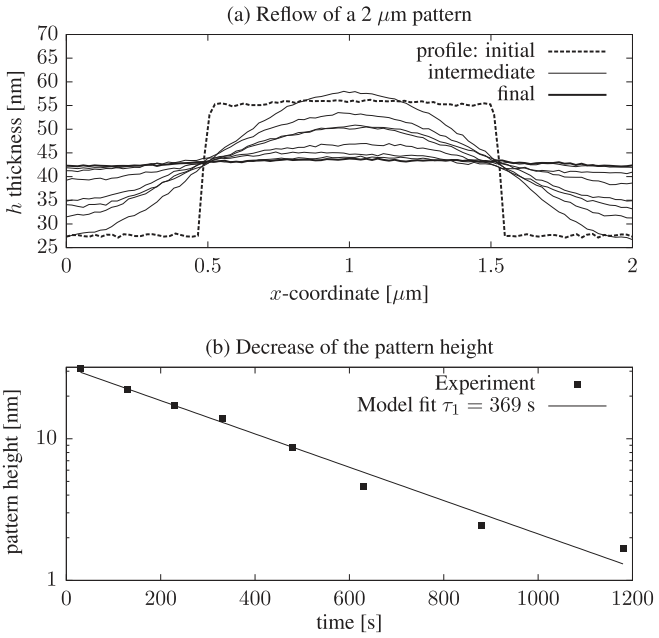

Fig. 3. Reflow of a 2 μm line grating. The annealing experiments were performed at 145 °C ($T_g + 43$ °C) between 50 and 1200 s. (a) AFM (3D and 2D) cross section profile evolution of the pattern. (b) Decrease of the pattern height fitted with the spectral model.

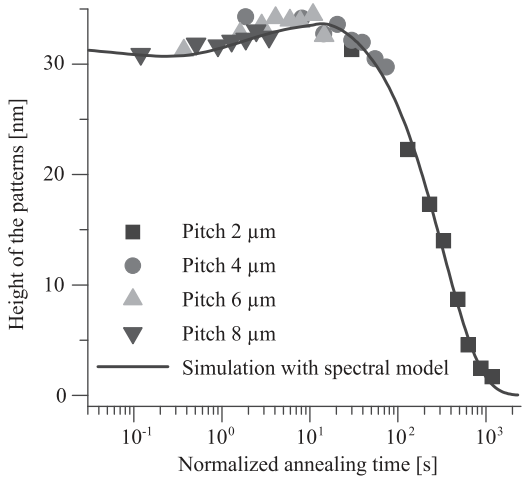

Fig. 4. Height evolution of the pattern for an annealing process ranging from 50 up to 1200 s. The real annealing times for the 4, 6 and 8 μm are normalized by the factors $1/2^4$, $1/3^4$, and $1/4^4$, respectively. The annealing temperature is $T_g + 43$ °C.

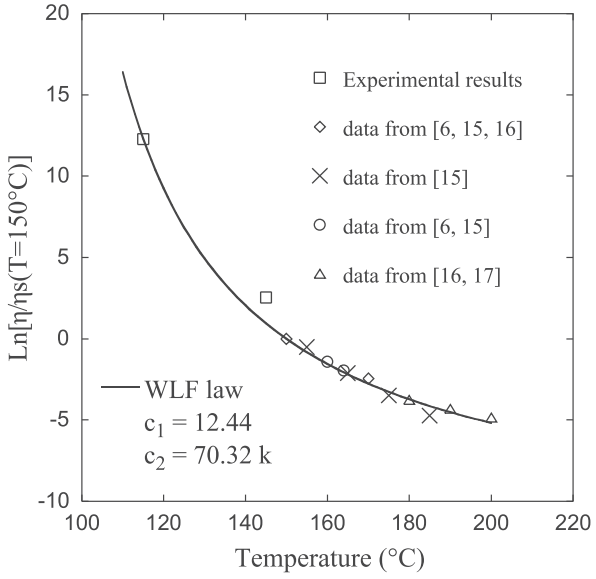

Fig. 5. Normalized polymer viscosity evolution versus temperature. Data from Refs. [6,15–17] and with different molecular weight were first normalized using the scaling law Eq. (8) and then data was normalized by the viscosity value at 150 °C. WLF law with c_1 and c_2 parameters equal to 12.44 and 70.32 K, respectively, is also plotted.

8 μm line grating) to 1200 s. On the same figure, the spectral model is represented making use of the time scale $\tau_1 = 369$ s. The pattern amplitude evolution is well described by our spectral approach with a correlation coefficient of 0.97 over the whole profile. This demonstrates that our approach allows us to describe any reflowing shapes even at early annealing time, which was not possible with previous works.

The viscosity of polymer melts can be extracted using the previously described technique at various temperatures. A similar experiment was performed at $T_g + 15$ °C and exhibits a much higher viscosity. This thermodependence of viscosity corresponds to a well-known behavior of a polymer material validated at macroscopic scale (polymer bulks). Extensively studied by William et al. [14], these authors proposed a constitutive law well adapted to describe thermal behavior for most of amorphous polymers:

$$\frac{\eta(T)}{\eta_s} = \exp\left(-c_1 \frac{T - T_s}{c_2 + T - T_s}\right) \tag{8}$$

with c_1 and c_2 two parameters and η_s the dynamic viscosity at the temperature T_s. Results are summed up in Fig. 5 and are consistent with data from previous authors.

5. Conclusion

In this paper, we proposed a new and accurate approach for direct polymer thin film viscosity measurement. We monitor pattern reflow manufactured by NanoImprint lithography to extract the PS viscosity from relaxation kinetic. Using PS films thick enough compared to pattern height, low molecular weight and low imprint-induced stresses, we demonstrated that even the first-stages of reflow were faithfully described by a dedicated viscous model. Our results clearly demonstrate that the whole reflow process is dominated by viscous damping. With the spectral analysis of the reflow dynamics proposed in this paper, we show that this approach provides two main advantages: first, whatever the initial surface shape is, the spectral decomposition of topography can be computed; and then, whatever the pattern wavelength and film thickness are, the decay time of the reflow process can be deduced from the quasi-ideal configuration of long-time reflow of iso-dense patterns. As a consequence, viscous reflow of organic or mineral material may be rigorously computed and profile evolutions can be predicted with a very high precision within an error less than 3%. As a way to validate this new methodology, we determine the viscosity of a low molecular weight (27.5 kg/mol) thin PS film (from 27 up to 237 nm) at a different temperature and we find good agreement with WLF law and data in literature.

References

[1] A. Oron, S. Davis, S. Bankoff, Rev. Mod. Phys. 69 (1997) 931–980.
[2] T. Leveder, S. Landis, L. Davoust, N. Chaix, Microelectron. Eng. 84 (2007) 953–957.
[3] R. Jones, T. Hu, C. Soles, E. Lin, R. Reano, S. Pang, D. Casa, Nano Lett. 6 (2006) 1723–1728.
[4] K. Petersen, D. Johannsmann, J. Non-Crystal. Solids 307 (2002) 532–537.
[5] D. Lumma, L. Lurio, S. Mochrie, M. Sutton, Rev. Scientific Instrum. 71 (2000) 3274.
[6] H. Kim, A. Rnhm, L. Lurio, J. Basu, J. Lal, D. Lumma, S. Mochrie, S. Sinha, Phys. Rev. Lett. 90 (2003) 68302.
[7] F. O'Neill, C. Walsh, J. Sheridan, Proceedings of SPIE 5456 (2004) 197.
[8] S. Chou, P. Krauss, P. Renstrom, Appl. Phys. Lett. 67 (1995) 3114.
[9] S. Landis, N. Chaix, C. Gourgon, C. Perret, T. Leveder, Nanotechnology 17 (2006) 2701.
[10] G. Dahlen, M. Osborn, N. Okulan, W. Foreman, A. Chand, J. Foucher, J. Vacuum Sci. Technol. B: Microelectron. Nanometer Struct. 23 (2005) 2297.
[11] T. Leveder, S. Landis, L. Davoust, App. Phys. Lett. 92 (2008) 013107.
[12] J. Israelachvili, Intermolecular and Surface Forces, Academic Press, London, 1991.
[13] J. Brandrup, E. Immergut, Polymer Handbook, third ed., John Wiley & Sons, New York, 1989.
[14] M. Williams, R. Landel, J. Ferry, J. Amer. Chemical Soc. 77 (1955) 3701–3707.
[15] J. Masson, P. Green, Phys. Rev. E 65 (2002) 31806.
[16] H. Schulz, M. Wissen, N. Bogdanski, H. Scheer, K. Mattes, C. Friedrich, Microelectron. Eng. 78 (2005) 625–632.
[17] C. Li, T. Koga, C. Li, J. Jiang, S. Sharma, S. Narayanan, L. Lurio, X. Hu, X. Jiao, S. Sinha, et al., Macromolecules 38 (2005) 5144–5151.